Shear behavior of high-strength self-compacting concrete beam-column joint panels

Mohammad Soleymani Ashtiani[1] and Rajesh P. Dhakal[2] and Allan N. Scott[3]

[1] *PhD research student, Department of Civil and Natural Resources Engineering, University of Canterbury, Private Bag 4800, Christchurch - 8140, New Zealand*
ms.ashtiani@pg.canterbury.ac.nz OR ms.ashtiani81@gmail.com
[2] *Associate professor, Department of Civil and Natural Resources Engineering, University of Canterbury, Private Bag 4800, Christchurch - 8140, New Zealand*
rajesh.dhakal@canterbury.ac.nz
[3] *Lecturer, Department of Civil and Natural Resources Engineering, University of Canterbury, Private Bag 4800, Christchurch - 8140, New Zealand*
allan.scott@canterbury.ac.nz

ABSTRACT:
The capability of self-compacting concrete (SCC) in flowing through and filling in even the most congested areas of reinforced concrete (RC) structures makes it ideal for being used in congested RC structural members such as beam-column joints (BCJ). However, members of tall multi-storey structures impose high capacity requirements where implementing normal-strength self-compacting concrete is not preferable. In the present study, a commercially reproducible high-strength self-compacting concrete (HSSCC) mix was designed using locally available materials in Christchurch, New Zealand. For comparison, a conventionally vibrated high-strength concrete (CVHSC) mix of equivalent compressive strength was also developed. Three beam-column joints (two HSSCC and a CVHSC) were designed following the guidelines of the New Zealand concrete standards NZS3101. Out of the two HSSCC subassemblies, one was designed using about half of the required joint shear reinforcement to investigate the relative contribution of concrete and joint shear reinforcement on the shear resistance of HSSCC beam-column subassemblies. All three BCJs were tested under a displacement-controlled quasi-static reversed cyclic regime. The cracking pattern at different load levels and the mode of failure are recorded. However, the measured load, displacement, drift, ductility, joint shear deformations, and elongation of the plastic hinge zone are also presented in this paper. It is found that none of the seismically important features are compromised by using HSSCC.

Keywords: beam-column joint, cyclic, high-strength, self-compacting concrete, shear

INTRODUCTION

Due to its special fresh and mechanical properties, Self-compacting concrete (SCC) has been regarded as one of the most important advances in concrete technology after its advent more than two decades ago. It has a unique ability to flow into a uniform level under the influence of gravity with the ability to compact by means of its self-weight without any internal or external vibration. Based on its exceptional flowing properties, SCC is able to be implemented in complex formworks even in highly congested reinforced concrete (RC) members. Therefore, the interest in utilizing SCC in members of concrete framed structures has increased manifold over the recent years.

The intersection of beams and columns represents one of the most congested parts of RC framed structures. Placing and consolidating concrete in such areas has often imposed difficulties which results in imperfect compaction and/or segregation of concrete. This entails other side effects such as deteriorated bond properties which later on associates with provision of more column depth than otherwise required in many of the RC standards. The capability of SCC in flowing through and filling in even the most congested areas makes it ideal for being used in congested RC members such as beam-column joints (BCJ) of high-rise buildings. However, members of tall multi-storey structures impose high capacity requirements where implementing normal-strength self-compacting concrete (NSSCC) is not preferable. At the same time, BCJs are subjected to enormous shear forces between the top and bottom beam bars which requires large amount of shear reinforcement. Therefore considering the advantages of HSSCC (noise reduction, reduced labour force, higher material quality and better surface finish) over conventionally vibrated concrete (CVC), if the seismic performance is not compromised, the implementation of HSSCC in BCJs could be an answer to all of the mentioned problems (i.e. compaction, bond and shear requirements).

Literature shows extensive investigations on fresh and mechanical properties (compressive, splitting tensile, and flexural strengths as well as modulus of elasticity, shrinkage and bond strength) of SCC including their comparison with that of CVC[1-7]. In addition, researchers have been working on the structural performance in RC members cast with SCC under monotonic loads in the past few years[8-10]. Nevertheless, to the best of the authors' knowledge only a few researchers have looked into the seismic behaviour of reinforced concrete beam-column joints cast with SCC[11] let alone HSSCC. Following the Canadian and American standards, Said et al[11] fabricated a SCC exterior beam-column joint with 28-day compressive strength of 50 MPa and investigated its performance under reversed cyclic loading. They also compared the behaviour of the SCC joint with that of a CVC benchmark specimen of the same concrete compressive strength range. They reported that the SCC specimen showed comparable cracking behaviour, load and displacement capacities and mode of failure to that of CVC up to 4.5% drift after which a faster reduction in load carrying capacity for SCC was observed. They attributed this to the lower coarse aggregate content in SCC which results in lesser friction due to aggregate interlocking; thus smaller contribution in the total shear resistance mechanism especially at the higher drifts. This was also reported to have resulted in a lower concrete contribution towards shear resistance in the beam for SCC specimen compared to that of CVC.

In the present study, a commercially reproducible HSSCC mix (100 MPa compressive strength) was designed using locally available materials in Christchurch, New Zealand. For comparison, a conventionally vibrated high-strength concrete (CVHSC) mix of equivalent compressive strength was also developed. Three beam-column joints (two of HSSCC and one of CVHSC) were designed following the guidelines of the New Zealand concrete standards NZS3101. Out of the two HSSCC subassemblies, one was designed using about half (56% to be precise) of the required joint shear reinforcement to investigate the relative contribution of concrete and joint shear reinforcement on the shear resistance of HSSCC beam-column subassemblies. All specimens were instrumented with linear variable displacement transducers (LVDT) on the joint and beam regions, strain gauges on both longitudinal and transverse reinforcements at different locations, load-cells at the lateral loading point and beam tips and pressure transducer at the hydraulic jack pipeline to measure the column axial load. All three BCJs were tested under a displacement-controlled quasi-static reversed cyclic regime. Recorded data was used to calculate the load vs. displacement, ductility, beam elongation, stiffness degradation, energy dissipation, deformation of the components and the joint, and contribution of steel and concrete in the joint shear stress. The experimental results of this study were used in identifying the pros and cons of using HSSCC in beam-column joints of the RC structures.

SPECIMEN PROPERTIES AND TEST SETUP

In the present investigation, locally available materials in Christchurch, New Zealand were used in order to design different concrete mixes; namely two HSSCC and a CVHSC (Table 1). Details of physical properties of the cement, fly ash, and aggregates as well as the mixing method and procedure are described in a previous study[2].

Table 1 — Different concrete mix proportions and properties

	HSSCC BCJ1	HSSCC BCJ3	CVHSC BCJ5
Coarse aggregate (kg/m^3)	880	880	1145
Fine aggregate (kg/m^3)	870	870	695
Cement (kg/m^3)	385	385	385
Fly ash (kg/m^3)	165	165	165
Water (kg/m^3)	165	165	148.5
Super-plasticizer (kg/m^3)	3.58	3.58	1.93
w/b ratio (designed)	0.30	0.30	0.27
w/b ratio (actual)	0.28	0.32	0.29
Slump (mm)	600*	700*	150
Compressive strength (MPa)	124.3	101.1	82.5
Splitting tensile strength (MPa)	7.0	7.4	6.5

*Slump-flow diameter was measured for HSSCC

Three standard beam-column joints, namely BCJ1 and BCJ3 (HSSCC) and BCJ5 (CVHSC), were designed following the current New Zealand Standard[12] requirements to achieve a strong-column-weak-beam hierarchy where the final expected mode of failure was hinging of the beam at the column face. Based on capacity design principals, column was designed to remain elastic throughout the test; this was ensured by keeping the ratio of the factored yield moment of the column (φM_y) to the over-strength moment of the beam ($M_{o,b}$) well above 1.0 for all specimens. The detailing of the reinforcement was identical in all three specimens except for the amount and type of joint shear reinforcement in BCJ3 (Figure 1). Ratios of the longitudinal reinforcement in the beam (tension side) and column were 0.011 and 0.025, respectively which were within the limits specified by the New Zealand Standard[12].

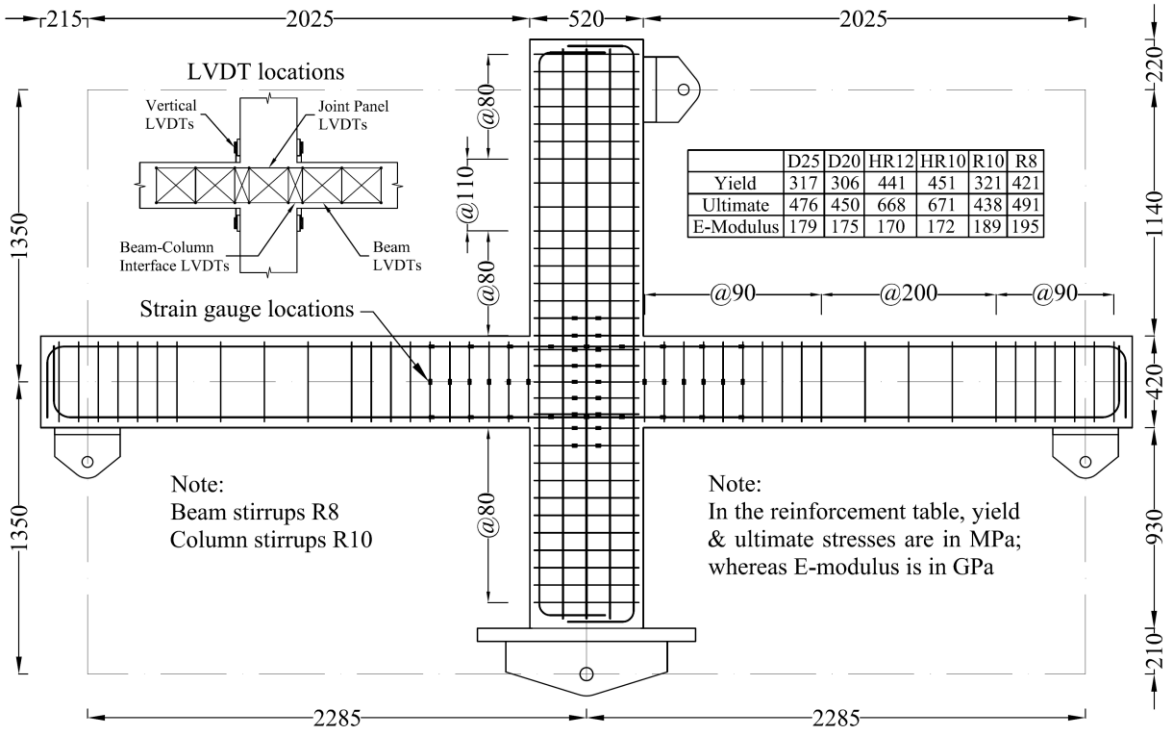

	D25	D20	HR12	HR10	R10	R8
Yield	317	306	441	451	321	421
Ultimate	476	450	668	671	438	491
E-Modulus	179	175	170	172	189	195

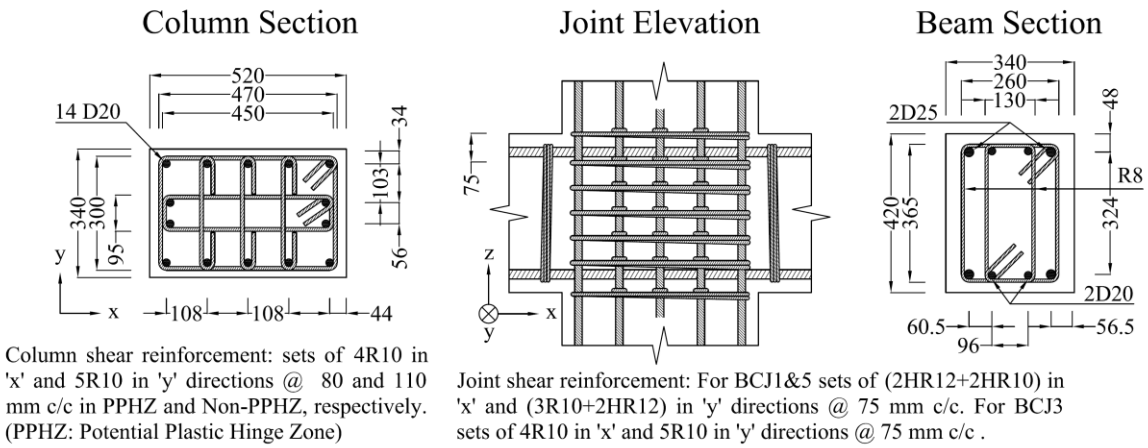

Figure 1 — Details of the beam-column subassemblies and instrumentations (dimensions are in 'mm')

In order to measure the local strains, strain gauges with 3 mm gauge length were installed on the top and bottom longitudinal beam bars as well as the shear reinforcement in the joint, beam and column (only the two stirrups adjacent to the joint). In addition, the beam plastic-hinge zone, beam-column interface and the joint panel were instrumented with LVDTs (installed on the surface) in order to measure the average strains, beam flexural and shear deformations, plastic-hinge zone elongation and joint shear deformations. It should be noted that as the column was designed to remain elastic, monitoring its deformations were not necessary; thus it was not instrumented with LVDTs or strain gauges (Figure 1). The lateral load was applied to the top of the column through a 400 kN capacity hydraulic actuator (ram) and measured using a load-cell. The ram was supported on the west by a strong reaction frame designed to take twice the actuator maximum capacity. The displacement was fed to the hydraulic actuator through a portable computer and associated controller. This was measured with a rotary potentiometer (located at the level of the actuator) which was connected to an independent frame to make sure that any slack in the setup did not affect the loading history. The designed axial load was applied through a 2500 kN capacity hydraulic jack and transferred to the column through the top and bottom plates and Macalloy bars. The bottom of the column and beam-ends were fixed to the strong floor using a pin and two roller supports, respectively. The generated loads at the end of the beams were measured using two load-cells. Figure 2 shows a schematic view of the setup used to test the beam-column subassemblies. A quasi-static displacement-controlled loading regime (Figure 2b) was adopted following the ACI guidelines for moment resisting frames[13]. The positive (+) and negative (-) drift directions were chosen based on the sign convention given in Figure 2a. Up to the 0.5% drift cycles, displacement increments of 0.5 mm were used in each loading step; however 1 mm increments were used for the rest of the cycles. Each displacement cycle was repeated 3 times and starting after the 0.5% drift cycle, a small cycle (1/3 magnitude of the preceding one) followed each cycle set.

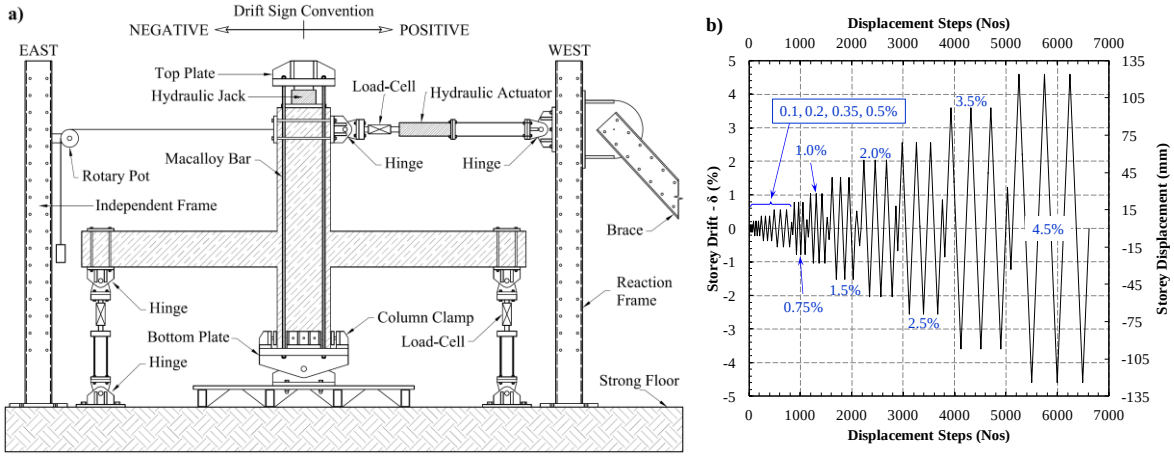

Figure 2 — a) Schematic view of the test setup and b) Applied displacement history

RESULTS AND DISCUSSIONS

The axial load was monitored and maintained throughout the test (using a pressure transducer) such that the axial load to capacity ratio remained almost the same for all specimens (0.07, 0.08 & 0.1 for BCJ1, BCJ3 and BCJ5, respectively). The test was paused at both '+' and '-' peaks of the 3rd cycle of each drift set. At each pause, cracks were marked and labelled with the drift, crack-widths were measured (using a hand microscope of 0.01 mm accuracy) and pictures were taken of the overall specimen and different damaged parts. In order to follow the crack patterns more efficiently, two grids of size 65 mm and 100 mm were drawn on the joint and beam surfaces, respectively. A test report was completed at every pause in order to associate the observations and manually collected data.

Hysteretic response and physical observations

Figures 3a-c show the storey shear versus drift response for the three specimens tested. The yield and test-end points (including displacement 'Δ', drift 'δ', and the storey shear) are annotated based on the test observations and the change in stiffness. The horizontal solid lines in Figure 3 (just above the yield points) show the predicted shear strength of the specimens calculated based on the factored nominal moment capacity of the beam (φM_n). Based on the ACI recommendations[13] the limiting drift value for the RC moment resisting frames is 3.5%. However, the adopted test setup in this study limited the maximum applicable drift to 4.5%, and none of the specimens had failed when the test was terminated after applying the 4.5% drift cycles. The measured drift values were converted to equivalent ductility (μ) defined as the ratio of drift (δ) at any stage to the drift at yield (δ_y); this is illustrated on a secondary axis parallel to the drift axis in Figure 3. According to the hysteresis loops for an identical ultimate drift of 4.5%, all three BCJs proved to be almost equally ductile. This contradicts the general notion that high-strength concrete (HSC) behaves in a brittle manner; in fact the better bond between concrete and reinforcement resulted in higher strain compatibility between the two materials; resulting in a relatively high ductility.

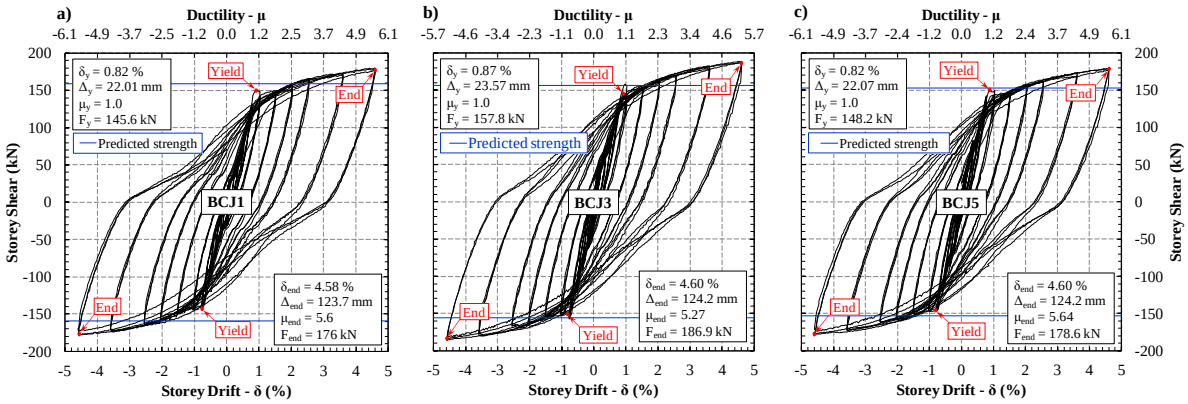

Figure 3 — Storey shear vs. drift response of all specimens

Figure 4 shows the physical condition of the joint in different specimens at positive drift ratios of 2.5% and 4.5%. It is clear from the pictures that the BCJ5 (CVHSC) had slightly more cracks in the joint area compared to that of BCJ1 and BCJ3; however the final mode of failure in all three specimens was the hinging of the beam. Although the amount of shear reinforcement in BCJ3 was almost half of the required amount, no shear failure happened in this specimen. In fact, even the amount and width of shear cracks were similar to those in BCJ1 at identical drift ratios. Note that in BCJ1, the broken concrete pieces were forcibly removed from the top and bottom of the specimen; that's why the 4.5% drift picture of BCJ1 looks more deteriorated than BCJ3 and BCJ5.

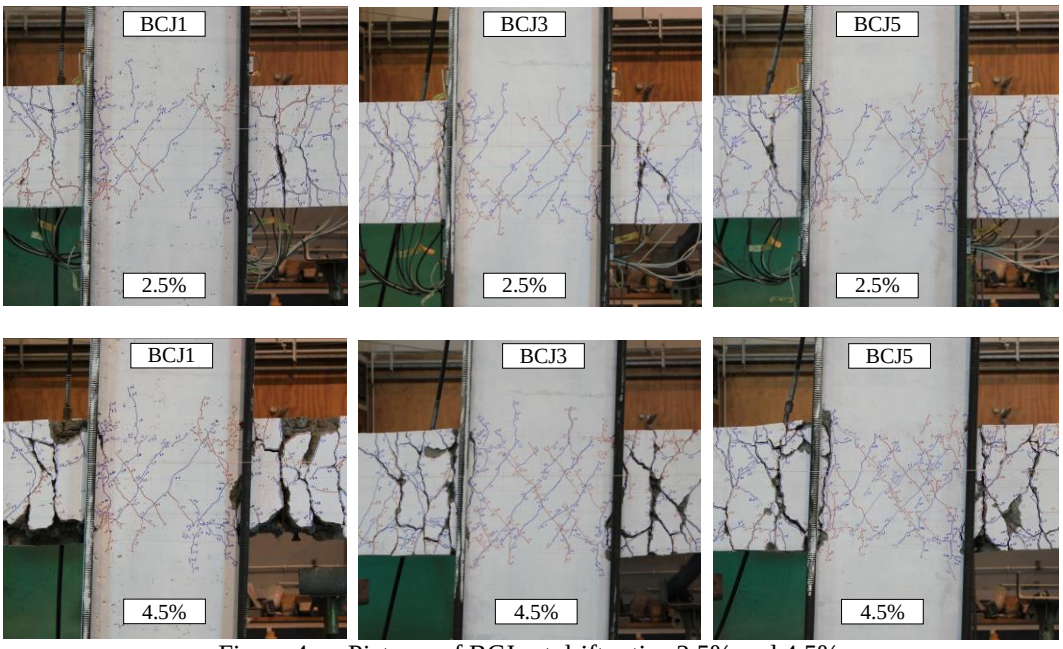

Figure 4 — Pictures of BCJs at drift ratios 2.5% and 4.5%

RESULTS AND DISCUSSIONS

The concept of energy dissipation was used to calculate the equivalent viscous damping for all specimens (Equation 1 to 3). This calculation was performed in order to provide a better understanding of the hysteresis and pinching behaviours. In addition, the peak-to-peak secant stiffness degradation was also calculated (Equation 4) for all specimens. Results of damping and stiffness degradation are shown in Figure 5.

$$\xi_{eq} = E_D / (4\pi.E_{sto}) \quad (1)$$

$$E_D = \Sigma (\Delta_{i+1} - \Delta_i) (F_i + F_{i+1}) / 2 \quad (2)$$

$$E_{sto} = F_0 \Delta_0 / 2 \quad (3)$$

$$k_p = (F_{+ve} - F_{-ve}) / (\Delta_{+ve} - \Delta_{-ve}) \quad (4)$$

In the above equations, 'ξ_{eq}' is the equivalent viscous damping, 'E_D' is the dissipated energy per cycle (N.mm), 'E_{sto}' is the equivalent elastic stored energy per cycle (N.mm), 'F_i' is the load at each step (N), 'Δ_i' is the displacement at each step (mm), 'F_0' is the peak load of each cycle (N), 'Δ_0' is the peak displacement of each cycle (mm), 'k_p' is the peak-to-peak stiffness (N/mm), 'F_{+ve}' and 'F_{-ve}' are the maximum and minimum forces of the intended cycle (N) and 'Δ_{+ve}' and 'Δ_{-ve}' are the maximum and minimum displacements of the intended cycle (mm).

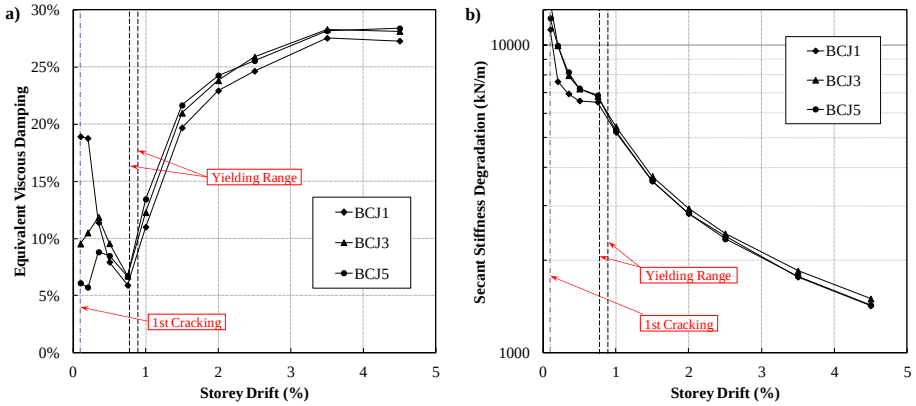

Figure 5 — a) Equivalent viscous damping and b) Peak-to-peak secant stiffness degradation

According to Figure 5 and based on the previous observations (Figure 3) at a given drift ratio after yielding, all three specimen show similar damping properties with only slight variations. Before yielding, BCJ1 shows considerably higher damping compared to the others; however these initially high values decrease quite fast so that the damping values become almost the same for all specimens around the yielding point. Note that the calculation of equivalent viscous damping requires division by the elastic stored energy 'E_{sto}', which is very small in the elastic response range; hence the calculated pre-yield damping values cannot be relied upon as they are very sensitive even to small discrepancies in estimating E_{sto}. Similarly in Figure 5b, all specimens show comparable stiffness degradation in the pre-yield range; with almost equal values after the yielding point. Note that the vertical axis in figure 5b is drawn in logarithmic scale.

Joint shear response

The total joint shear force 'V_{jh}' and the horizontal joint shear stress 'v_{jh}' at each drift peak were calculated using the geometry of the test setup and specimens. The contribution of the joint shear reinforcement to the total joint shear stress was calculated using the results of the strain gauges installed on the joint stirrups (Figure 6). According to the strain gauge readings, even at the highest storey drift of 4.5% none of the joint stirrups yielded. In fact they all remained elastic around half-yield levels except for the joint shear reinforcement of BCJ3 which passed the half-yield point but remained elastic. Therefore stresses were calculated using Hooke's law and the corresponding forces were determined by multiplying the stresses and the area of stirrups. Shear stress of the joint was also normalized with respect to the square root of concrete compressive strength '$\sqrt{f'_c}$' to provide an unbiased assessment of the steel and concrete contributions to the total joint shear stress (Figure 7). Despite the joint shear stress being similar in the three specimens, the steel contribution to joint shear was more in BCJ3 compared to that in BCJ1 and BCJ5. This is attributed to the lower amount of shear reinforcement in the former (only 56% of the required amount based on code recommendations). The maximum limit of joint shear stress for all specimens, calculated as per the American and New Zealand standards[12, 14] are also shown in Figure 7 for comparison. As mentioned earlier, all specimens were designed to the New Zealand Standard[12], therefore it was expected that the maximum joint shear stress would not exceed the codal limits.

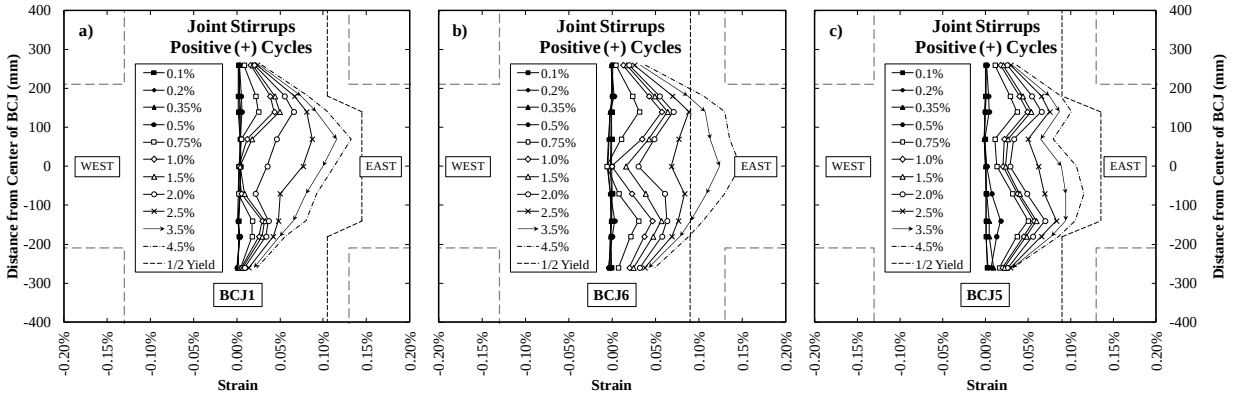

Figure 6 — Strain profile of the joint shear reinforcement at different drift levels

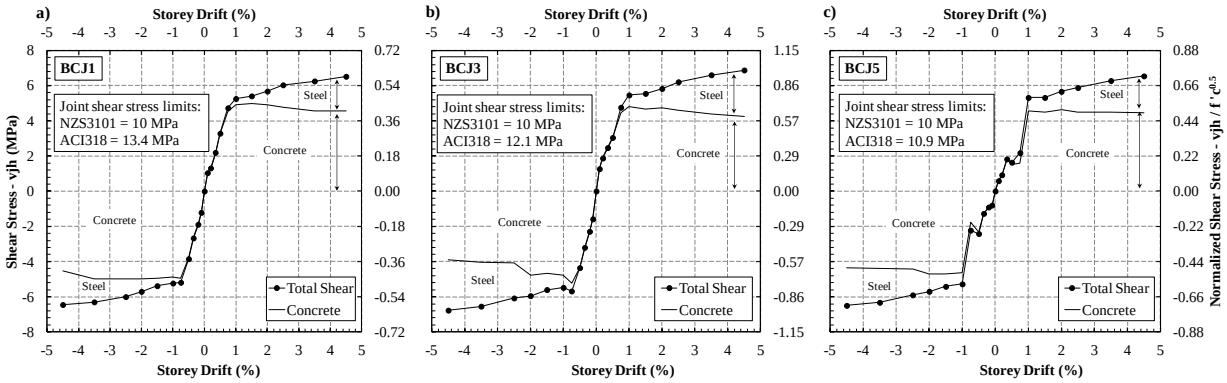

Figure 7 — Contribution of concrete and steel in joint shear capacity

The overall deformation of a beam-column subassembly comprises of beam, column and joint deformations. As the specimens were designed to fail by the formation of plastic hinge in the beam region, the beam deformation would be contributed by four different components: elastic flexure, fixed-end rotation (i.e. cracking), plastic hinge rotation and shear deformations. On the contrary, as the column was designed to remain elastic throughout the test, the column deformation comprises only of the elastic flexure and shear deformations. It should be mentioned that the beam and column shear deformations were considerably small compared to the other components; hence they were neglected. Finally, the joint contribution to the overall deformation comes solely from the shear deformation of the joint panel. Figure 8 shows the contributions of the different elements (beam, column and joint) to the overall displacement of each specimen at the peak drifts. As could be expected based on the designed failure mode (beam hinging), the beam contributed considerably more towards the overall specimen drift than the column and the joint did. The contributions of the column and joint were almost identical in all three specimens.

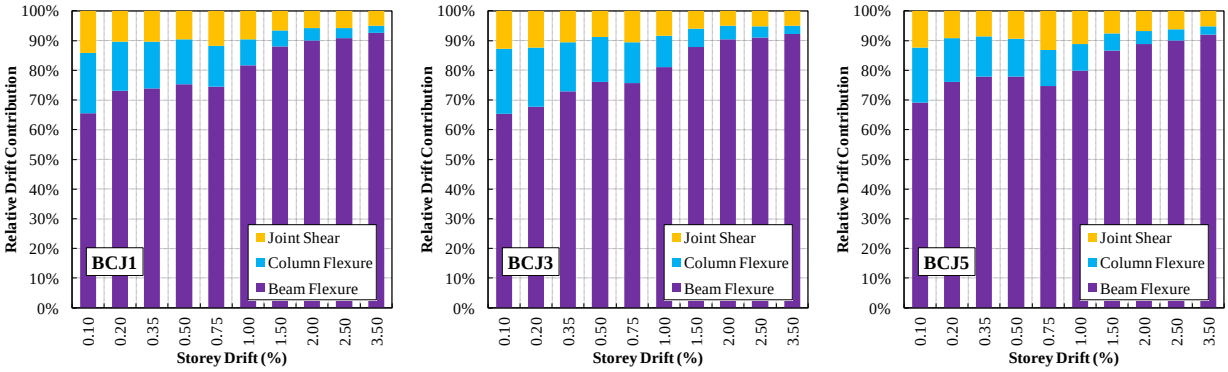

Figure 8 — Relative contributions of different components to the overall specimen drift

Beam elongation

Using the LVDTs installed on the surface of specimens, the elongation of the plastic hinge zone was also calculated for the west and east beams. Total elongation (sum of the west and east) of each specimen is shown in Figure 9. A closer look at the elongation graphs reveals that before yielding the elongation was very small and reversible to zero for all specimens. However, it started to increase and become irreversible in nature at higher drifts (after yielding). This can be explained by the fact that when the specimens were in their elastic response region, the cracks were small and closed completely during unloading; consequently the elongations were small and reversible. However when the cracks started to widen in the larger post yield drift cycles, small pieces of concrete dropped into the void created by the cracks. In the reverse cycle, these concrete parts started transferring the forces from one side of the crack to the other before these cracks closed completely. As a result, the reinforcement in the tension side started elongating before the cracks on the compression side fully closed down. This caused the cracks to open up in the next cycle even more and this continued throughout the loading regime; thereby gradually increasing the permanent elongation of the plastic hinge zone. In addition to the explained phenomenon, plastic strain of the top and bottom

beam bars after yielding may also have added to the overall elongation of the plastic hinge zone. As can be seen in the figures, all three specimens elongated to similar extent; the total elongation (after 3.5% drift) was about 30 mm; which is more than 7% of the beam depth.

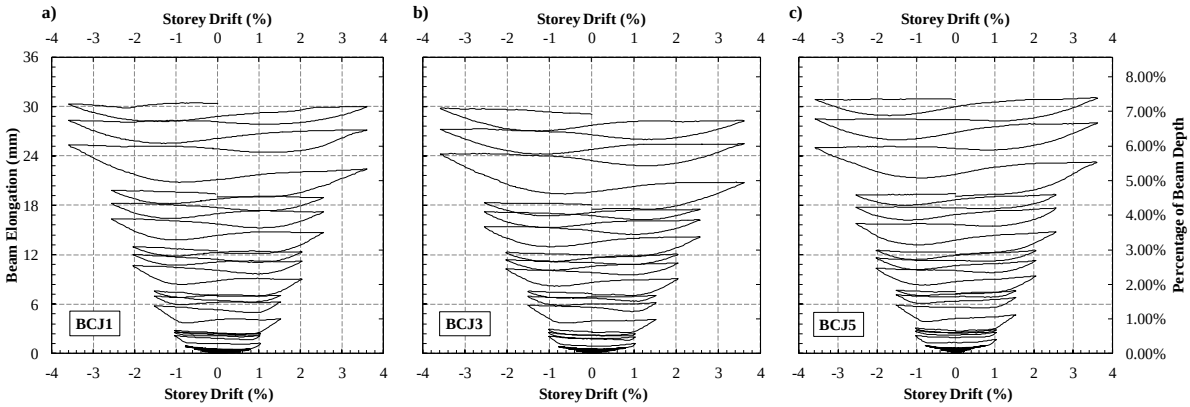

Figure 9 — Total elongation of the plastic hinge zone (west and east beam)

CONCLUSIONS

Based on the cyclic test results of the three specimens reported in this study, following conclusions are drawn:

- At a given drift ratio, more cracks had appeared in the joint area of the CVHSC specimen compared to the other two HSSCC ones. Higher compressive strength of the HSSCC and stronger bond were the main reasons for this.
- All specimens showed a relatively high ductile behaviour as opposed to the general notion of brittle failure in HSC. This can be attributed to the better strain compatibility between HSC and reinforcing steel.
- As indicated by the pinched hysteretic loops, all specimens showed comparable damping properties irrespective of being CVHSC or HSSCC.
- Except for very slight variations, the stiffness degradation was similar amongst all specimens.
- Except for slight variations, the relative contribution of joint shear reinforcement and concrete in the joint shear stress was similar amongst the HSSCC and CVHSC specimens. As expected, the joint stirrups in the HSSCC specimen with a lower quantity of shear reinforcement experienced higher strain compared to the other two specimens. However, the joint stirrups remained well below the yielding level in all specimens. As expected, the maximum shear stress in the joint remained within the allowable standard limits.
- It was observed that the beam contributed the most towards the specimen overall drift in all three specimens; the contribution of column and joint were very small compared to that of the beam. Here too apart from slight discrepancies, the overall trend was similar amongst all specimens.
- The beam elongation trends of all specimens were similar; the maximum total elongation (at 3.5% drift) was more than 7% of the beam depth (i.e. about 30 mm).
- Overall, seismic behaviour of the HSSCC and CVHSC specimens were quite similar and none of the key parameters related to seismic performance were compromised by using HSSCC. In fact the better bond properties and very high compressive strength resulted in lesser requirement of joint reinforcement. Hence, HSSCC may offer an easier option (compared to CVC) for heavily congested areas like beam-column connections in RC frame structures.

As mentioned previously, the amount of research on the seismic performance of SCC is very limited in the accessible literature and there is no information available on the cyclic behaviour of HSSCC under earthquake type excitations. It should be noted that the findings and recommendations of this study were based on a limited number of laboratory experiments conducted on HSSCC and CHVSC beam-column joint subassemblies. Therefore, any further generalization of these results without stronger backing from more data is not encouraged. As the concept of HSSCC is relatively new in the field of structural engineering, more investigations are required in order to fully understand the complexities involved in the seismic performance of structural members cast with this special concrete type.

ACKNOWLEDGEMENT

The authors would like to extend their sincere thanks to Tim Perigo, technician of the structures laboratory at the University of Canterbury, for his continuous support throughout the experimental stage of this study. Without his diligent efforts and high-quality inputs, fabrication and testing of the beam-column subassemblies would have become a much more tedious task. Thanks are also due to Joe Byrne, ME student at the University of Canterbury, for his cooperation in fabricating the specimens.

APPENDIX

For simplicity and clarity of the paper, inclusion of double units (metric and English) in figures, graphs and tables is avoided. Instead the Table 2 provides the relevant conversion factors for the units used throughout the paper.

Table 2 — Conversion factors for metric and English units

Metric (SI) units		English (American customary) units	
1	millimeter (mm)	0.03937	inch (in)
1	meter (m)	3.28084	foot (ft)
1	kilogram (kg)	2.20462	pound (lb)
1	Newton (N)	0.22481	pound-force (lbf)
1	kilo-Newton (kN)	0.22481	kilo-pound-force (kips)
1	kilo-Newton/meter (kN/m)	68.52176	pound-force/foot (lbf/ft)
1	mega Pascal (MPa)	145.03774	pound-force/ square inch (psi)
1	giga Pascal (GPa)	145.03774	kilo-pound-force/ square inch (ksi)
1	kilogram/cubic meter (kg/m^3)	0.062428	pound/cubic foot (lb/ft^3)

REFERENCES

1. Soleymani Ashtiani, M.; R.P. Dhakal; and A.N. Scott, "Bond properties of reinforcement in high-strength self-compacting concrete", in *Proceedings of the 9th Symposium on High Performance Concrete Design, Verification and Utilization*, 2011, Rotorua, New Zealand.
2. Soleymani Ashtiani, M.; A.N. Scott; and R.P. Dhakal, "Mechanical properties of high-strength self-compacting concrete", in *Proceedings of the 21st Australasian Conference on the Mechanics of Structures and Materials*, 2010, Melbourne, Australia.
3. Desnerck, P.; G. De Schutter; and L. Taerwe, "Bond behaviour of reinforcing bars in self-compacting concrete: Experimental determination by using beam tests", *Materials and Structures/Materiaux et Constructions*, 2010, 43: pp. 53-62.
4. Valcuende, M. and C. Parra, "Bond behaviour of reinforcement in self-compacting concretes", *Construction and Building Materials*, 2009, 23(1): pp. 162-170.
5. De Almeida Filho, F.M.; M.K. El Debs; and A.L.H.C. El Debs, "Bond-slip behavior of self-compacting concrete and vibrated concrete using pull-out and beam tests", *Materials and Structures/Materiaux et Constructions*, 2008, 41(6): pp. 1073-1089.
6. Domone, P.L., "Self-compacting concrete: An analysis of 11 years of case studies", *Cement and Concrete Composites*, 2006, 28(2): pp. 197-208.
7. Persson, B., "A comparison between mechanical properties of self-compacting concrete and the corresponding properties of normal concrete", *Cement and Concrete Research*, 2001, 31: pp. 193-198.
8. Hassan, A.A.A.; K.M.A. Hossain; and M. Lachemi, "Behavior of full-scale self-consolidating concrete beams in shear", *Cement and Concrete Composites*, 2008, 30(7): pp. 588-96.
9. Lachemi, M.; K.M.A. Hossain; and V. Lambros, "Shear resistance of self-consolidating concrete beams - Experimental investigations", *Canadian Journal of Civil Engineering*, 2005, 32(6): pp. 1103-1113.
10. Sonebi, M.; A.K. Tamimi; and P.J.M. Bartos, "Performance and Cracking Behavior of Reinforced Beams Cast with Self-Consolidating Concrete", *ACI Materials Journal*, 2003, 100(6): pp. 492-500.
11. Said, A. and M. Nehdi, "Behaviour of reinforced self-consolidating concrete frames", *Proceedings of the Institution of Civil Engineers: Structures and Buildings*, 2007, 160(2): pp. 95-104.

12. NZS3101, *Concrete structures standard Parts 1 & 2: The Desing of Concrete Structures and Commentary*, 2006, Standards New Zealand: Wellington, New Zealand. pp. 698.
13. ACI374.1-05, *Acceptance criteria for moment frames based on structural testing and commentary*, 2005, ACI Committee 374. pp. 9.
14. ACI318M-08, *Building Code Requirements for Structural Concrete and Commentary*, 2008, ACI Committee 318. pp. 479.